Cellulose (2019) 26:9095–9105
https://doi.org/10.1007/s10570-019-02716-2

ORIGINAL RESEARCH

Highly reversible photochromism in composite WO_3/nanocellulose films

O. L. Evdokimova · T. V. Kusova · O. S. Ivanova · A. B. Shcherbakov · Kh. E. Yorov · A. E. Baranchikov · A. V. Agafonov · V. K. Ivanov

Received: 16 June 2019 / Accepted: 23 August 2019 / Published online: 6 September 2019

Abstract Reversible photochromic hybrid organic–inorganic films containing nanocrystalline cellulose as a matrix and tungsten oxide as a photochromic component (CNC/WO_3) were obtained via a simple and quick solvent casting method. The films were studied by scanning electron microscopy, together with element mapping, FT-IR spectroscopy and X-ray diffraction, confirming successful incorporation of WO_3 nanoparticles into a nanocellulose matrix. Thermal analysis data indicated that the modification of a nanocellulose matrix with WO_3 increases its thermal stability. The CNC/WO_3 films showed a quick coloration-bleaching transition with good reversibility within 20 min, without notable degradation of photochromic properties after 10 cycles. The synthetic method proposed allows for scalable preparation of highly efficient low-cost WO_3-based photochromic materials.

Electronic supplementary material The online version of this article (https://doi.org/10.1007/s10570-019-02716-2) contains supplementary material, which is available to authorized users.

O. L. Evdokimova · T. V. Kusova · A. V. Agafonov (✉)
Krestov Institute of Solution Chemistry of the Russian Academy of Sciences, Ivanovo, Russia 153045
e-mail: ava@isc-ras.ru

O. L. Evdokimova · T. V. Kusova · O. S. Ivanova · A. E. Baranchikov · V. K. Ivanov
Kurnakov Institute of General and Inorganic Chemistry of the Russian Academy of Sciences, Moscow, Russia 119991
e-mail: a.baranchikov@yandex.ru

A. B. Shcherbakov
Zabolotny Institute of Microbiology and Virology of the National Academy of Sciences, Kiev 03143, Ukraine

Kh. E. Yorov
Lomonosov Moscow State University, Moscow, Russia 119991

V. K. Ivanov
National Research Tomsk State University, Tomsk, Russia 634050

Graphic abstract

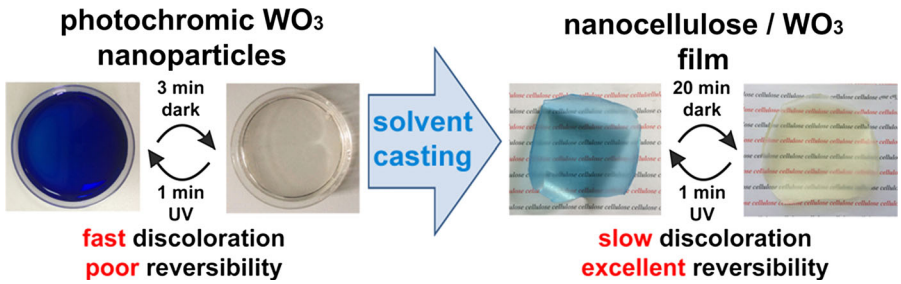

Keywords Nanocellulose · Tungsten oxide · Composite · Photochromism · Film

Introduction

In recent years, the development of hybrid organic–inorganic nanomaterials based on polymers and metal oxide nanoparticles has attracted a great deal of attention (Faustini et al. 2018). Being an easily available biopolymer, nanocellulose demonstrates remarkable physical properties, flexible surface chemistry, thermal stability and excellent biological properties (biocompatibility, biodegradability and non-toxicity) (Kaushika and Moores 2016; Siqueira et al. 2010). Integration of inorganic nanoparticles into the nanocellulose matrix is an excellent route for developing novel hybrid materials with advanced performance (Dong et al. 2013; Shi et al. 2013).

Among the various inorganic nanomaterials, tungsten oxide enjoys special interest, due to its low toxicity and good biocompatibility with human, animal and plant cells (Han et al. 2019; Chinde et al. 2017). The functional properties of WO_3-based nanomaterials are determined by numerous factors, including the electronic properties of WO_3 [band gap from 2.7 to 3.1 eV (Thummavichai et al. 2017)], the possibility of reversible W(V) ↔ W(VI) redox reactions, the diverse polymorphism of tungsten trioxide and its ability to form a wide variety of non-stoichiometric compounds (e.g., tungsten bronzes) (Bartha et al. 1995; Tahir et al. 2017). At present, nanocrystalline WO_3 is widely used in electrochromic, photochromic, and gasochromic devices (Zheng et al. 2011; Kalhori et al. 2016), photocatalytic systems for wastewater treatment and photoelectrochemical decomposition of water (Yamazaki et al. 2013; Nandiyanto et al. 2013), heterogeneous catalysts (Zhao et al. 2018), gas sensors (Siciliano et al. 2008; Shekunova et al. 2018), and contrast agents for computed tomography (Jakhmola et al. 2014). WO_3 nanoparticles are considered to be a promising component of multifunctional biomedical and photochromic nanocomposites. Recently, it was demonstrated that tungsten oxide can be applied as an antibacterial agent against gram positive and gram negative bacteria, for the photothermal destruction of malignant cells (Hosseini et al. 2018; Yassin et al. 2016) in exhaled breath sensors (Kim et al. 2016) etc.

The development of scalable production processes for WO_3-based materials with highly reversible photochromic properties that can easily be scaled-up for commercial purposes is a top priority for researchers worldwide (Wang et al. 2018). At present, the most common techniques for the production of films containing photochromic WO_3 nanoparticles are dip-coating deposition and electrodeposition (Shen et al. 1992) and hydrothermal deposition (Ding et al. 2012). Stoenescu et al. (2016) produced nanocellulose/tungsten oxide composites deposited on indium-tin-oxide(ITO)-coated substrates by dipping ITO glasses into a mixture of nanocellulose and peroxotungstic acid in water–alcohol media. Yamazaki et al. (2015) succeeded in the fabrication of photochromic films by incorporating WO_3 particles in a methylcellulose matrix, using different surfactants. Zhang et al. (2018) proposed a facile route to prepare cellulose-based WO_3 nanocomposites via a sol–gel method at a temperature of 100 °C. However, despite the enormous attention paid to the development of WO_3-based materials, flexible WO_3-containing composite films

made from nanocellulose remain completely unexplored and thus require thorough investigation. Previously, we have shown that the hydrothermal treatment of tungstic acid in the presence of polyvinyl pyrrolidone (PVP) allowed us to obtain ultra-small WO_3 nanoparticles ($\sim$ 2 nm) suitable for various photochemical applications (Popov et al. 2018). In this paper, a simple and quick solvent casting method was applied for the preparation of nanocellulose-based films loaded with polyvinyl pyrrolidone-coated WO_3 nanoparticles. These hybrid organic–inorganic films exhibited good mechanical flexibility and demonstrated reversible photochromic properties.

Experimental

Materials

All the chemicals were of an analytical grade and used without further purification. Sodium tungstate (Na_2WO_4), sodium hydroxide (NaOH), aqueous ammonia (NH_4OH, 25 wt%), polyvinyl pyrrolidone (PVP K-30, average mol. wt. 40,000), H_2SO_4 (purity 98%) were purchased from Sigma-Aldrich. Filter paper (Khimmed, GOST 12026-76) was used as a precursor material for cellulose nanocrystals (CNC) production.

Preparation of hybrid nanocellulose/WO_3 films

For the preparation of the hybrid CNC/WO_3 films, photochromic WO_3 nanoparticles synthesized via a low-temperature treatment of tungstic acid in the presence of PVP were used (Popov et al. 2018). Briefly, Na_2WO_4 0.03 M solution was passed dropwise through cation exchange resin (Amberlite® IR120) in H^+-form. Then, PVP was added to the eluent, and the solution was refluxed for 4 h.

Nanocrystalline cellulose (CNC) was obtained by the two-step process described in detail in our earlier paper (Evdokimova et al. 2018). The method included two steps, namely complexation with a copper (II) solution in aqueous ammonia (Cuam), followed by acid hydrolysis with diluted H_2SO_4 (20 wt%). Briefly, the Cuam solution was prepared by dissolving a freshly prepared copper hydroxide in ammonia (25 wt%). Then, the chosen amount of the filter paper was completely dissolved in the Cuam solution. Next, 25 mL of the Cuam solution, containing the dissolved filter paper, were added into 100 mL of 20 wt% of the sulfuric acid solution and stirred vigorously at 70 °C for 1 h. After that, hydrolysis was immediately quenched by adding 500 mL of cold water to the reaction mixture. The resulting nanocellulose slurry was separated from the sulfuric acid by several cycles of centrifuging and washing with distilled water until neutral pH was achieved, and then stored at 4 °C till further use.

The hybrid CNC/WO_3 film was produced by the addition of 1 ml of WO_3 sol (7 g L^{-1}) into nanocellulose slurry (8 g, 1.8 wt%) and 0.2 ml of glycerol as a plasticizer. The obtained suspension was vigorously stirred at 40 °C for 30 min. The resulting CNC/WO_3 sol containing $\sim$ 5 wt% of WO_3 was poured into a Petri dish and left in an oven at 40 °C for 72 h. The neat nanocellulose film (CNC) was also synthesized by an identical procedure in the absence of WO_3, but with the addition of the same amount of glycerol and PVP as the plasticizers. The thickness of the CNC/WO_3 film was about 0.22 mm.

Characterization

The morphology of the obtained samples was characterized by a Carl Zeiss NVision 40 scanning electron microscope (SEM) at an accelerating voltage of 1 kV. Energy-dispersive X-ray spectroscopy (EDX) was performed using an Oxford Instruments X-Max detector at 20 kV acceleration voltage. Before EDX measurements, a thin film of conductive carbon layer ($\sim$ 5 nm) was deposited on the surface of the sample. FT-IR spectra were recorded with a Bruker VERTEX 80 v FT-IR spectrometer (Germany) in absorbance mode in the range of 400–4000 cm^{-1}. All spectra were smoothed and baseline corrected. The X-ray diffraction (XRD) studies were carried out at room temperature, using a Bruker APEX II CCD diffractometer ($Cu_{K\alpha}$ radiation). Thermogravimetric analysis (TGA) of the composite films was carried out using a Netzsch STA 409 PC, in the temperature range of 25–600 °C, at a heating rate of 10 min $°C^{-1}$ in air.

Investigation of photochromic properties

The investigation of the photochromic properties of the hybrid films was carried out by irradiating the samples, using a 6 W UV lamp NU-6 KL (Konrad Benda Laborgeräte, Wiesloch, Germany). The

samples were directly exposed to UV light (at a wavelength of 366 nm) at room temperature, with a distance of 30 cm between the film (34 mm × 17 mm) and the UV source. The bleaching process was investigated in the dark at ambient temperature. The neat nanocellulose film was used as a control sample under both light and dark conditions. Neat WO_3 photochromic sol (0.5 g L^{-1}) was also used as a reference sample. The absorption spectra of the irradiated films were recorded in the range of 400–800 nm, using a PG Instruments T70 + UV/VIS spectrophotometer (PG Instruments Limited, Leicestershire, UK). Coloration and bleaching of the films were monitored by measuring absorption at 624 nm at regular intervals of time in a kinetic mode. To quantitatively describe the photochromic transition, the relative intensity (A_i/A_o) was calculated, where A_o and A_i were the absorbance values at 624 nm, obtained at t_o and t_i time.

Results and discussion

The characterization of the hybrid CNC/WO_3 films

Previously, we have shown that the hydrothermal treatment of tungstic acid in the presence of PVP allowed us to obtain ultra-small WO_3 nanoparticles (∼ 2 nm) (Popov et al. 2018); in turn, nanocellulose particles prepared by a solvent casting method possessed an average size of 25 nm (Evdokimova et al. 2018). According to SEM data (Fig. 1a, b), the pure nanocellulose film has a uniform and smooth surface, while the surface of hybrid CNC/WO_3 film has an increased roughness, due to the introduction of tungsten oxide nanoparticles into the nanocellulose matrix. Certain increases in CNC roughness upon the introduction of other types of nanoparticles (TiO_2) have also been observed in our recent work (Evdokimova et al. 2018). Apparently, such an effect may arise from the changes in the aggregation pattern of CNC particles. According to EDX measurements, tungsten oxide is uniformly distributed over the CNC matrix (Fig. 1c, d).

To investigate the possible interaction between nanocellulose and tungsten oxide nanoparticles, the obtained samples were analyzed using FT-IR spectroscopy. Figure 2a shows the FT-IR spectra of CNC and CNC/WO_3 films. The broad band in the 3600–3000 cm^{-1} region corresponds to the O–H stretching vibrations of the hydrogen bonded hydroxyl group in the cellulose molecules involved in intermolecular hydrogen bonds (Poletto et al. 2014). The presence of the absorption peak at 2900 cm^{-1} is attributed to the stretching vibrations of C–H groups of cellulose (Reddy and Rhim 2014). The peak at

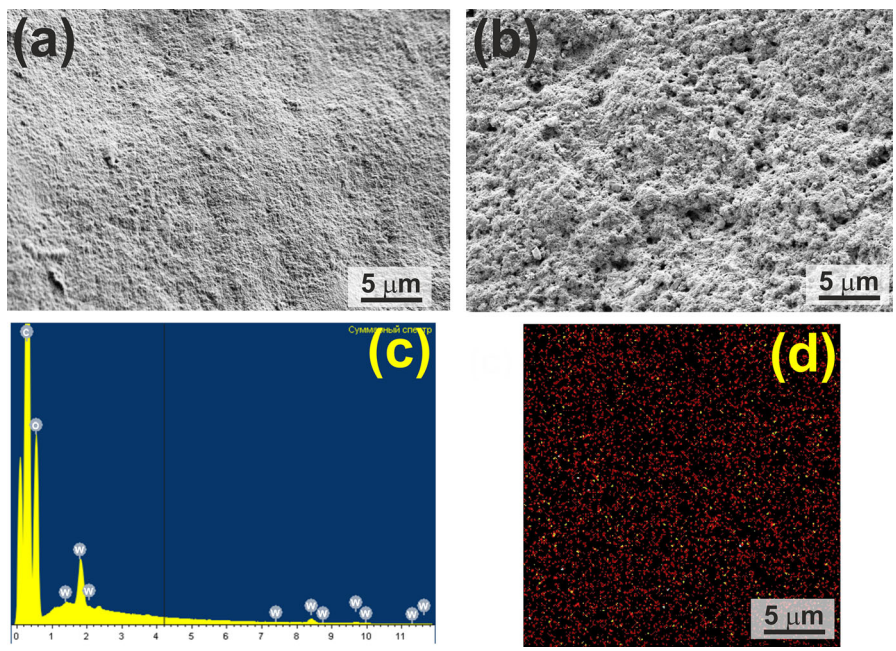

Fig. 1 SEM images of **a** CNC and **b** CNC/WO_3 films. EDX analysis **c** and element (W L_α) mapping of CNC/WO_3 film (**d**)

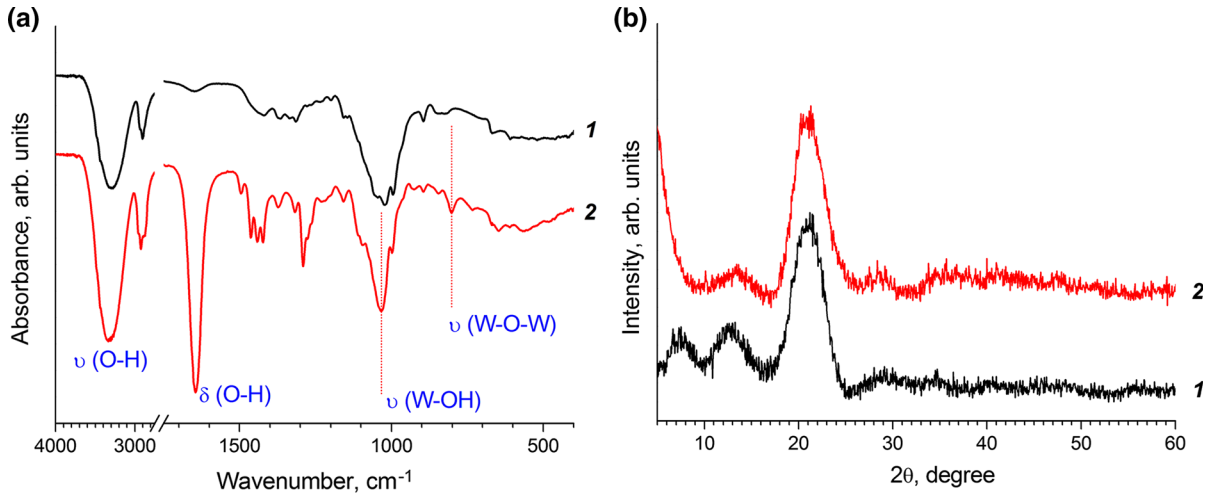

Fig. 2 **a** FT-IR spectra and **b** XRD patterns of (1) bare nanocellulose (CNC) and (2) hybrid CNC/WO_3 films

1016 cm^{-1} is related to the stretching vibrations of C–OH bonds. The absorption peak at 1644 cm^{-1} in both bare CNC and hybrid CNC/WO_3 films corresponds to H–OH bond bending vibration of the adsorbed water. Compared to the spectra of bare nanocellulose film without WO_3 loading, several new peaks were observed in the FT-IR pattern of CNC/WO_3, indicating the successful incorporation of WO_3 into the nanocellulose matrix. In particular, after WO_3 modification, a weak band at 802 cm^{-1} was observed assigned to the stretching vibration of W–O–W bonds. The peak at 1033 cm^{-1} is associated with the tungsten–hydroxide–water bonds (W–OH) stretching vibration (Dejournett and Spicer 2014).

The X-ray diffraction data showed that both CNC and hybrid CNC/WO_3 films have almost the same diffraction patterns (Fig. 2b). Bare nanocellulose film gives a diffraction pattern typical to crystalline cellulose II [characteristic diffraction peaks at $2\theta = 12.7°$ and 20.9°, corresponding to $(1\bar{1}0)$ and (110) reflections, respectively (Ling et al. 2017)]. Estimation of CNC particle size using the Scherrer formula resulted in ~ 2.5 nm value. For the CNC/WO_3 sample, the similar diffraction maxima were also observed at 12.7° and 20.9°. No additional peaks were registered for the hybrid CNC/WO_3 films as a result of WO_3 incorporation, the cellulose particle size also being the same (~ 2.5 nm). Note that in the diffraction pattern of the CNC/WO_3 sample, a notable rise of the baseline in a small-angle region is observed ($2\theta < 10°$), which can be attributed to the X-ray scattering on ultra-small X-ray amorphous tungsten oxide nanoparticles.

Taking into account the possible use of hybrid CNC/WO_3 films in biomedicine and the food packaging industry, their thermal stability was additionally studied, since both applications require a standard sterilization procedure (heating to 150 °C for 20 s at an atmospheric pressure) (Kuribara et al. 2012). The results of thermal analysis (thermogravimetric, TGA, and differential thermogravimetric, DTG, curves) for bare CNC and CNC/WO_3 demonstrate a complex weight loss behavior (see Fig. 3). At the first step of the decomposition (low temperature range, 25–180 °C), both samples showed a small weight loss of ~ 5–6% due to the evaporation of physically adsorbed water and intermolecular H-bonded water, as well as low molecular weight compounds remaining from the nanocellulose synthesis (Henrique et al. 2015). The major weight loss in all the samples occurred at 200–360 °C, corresponding to the thermal degradation of cellulose due to its oxidation, depolymerization, dehydration, as well as decomposition of glycosidic units (Henrique et al. 2015). According to DTG analysis, CNC and CNC/WO_3 showed a maximum thermal degradation temperature at 330 °C and 280 °C respectively. The differences in thermal decomposition behavior of the pure CNC and CNC/WO_3 samples in the temperature range of 300–500 °C obviously arise from the complex oxidation behavior of WO_3/cellulose composite material. Fast heating (10 °C min^{-1}) of WO_3 with cellulose results in the

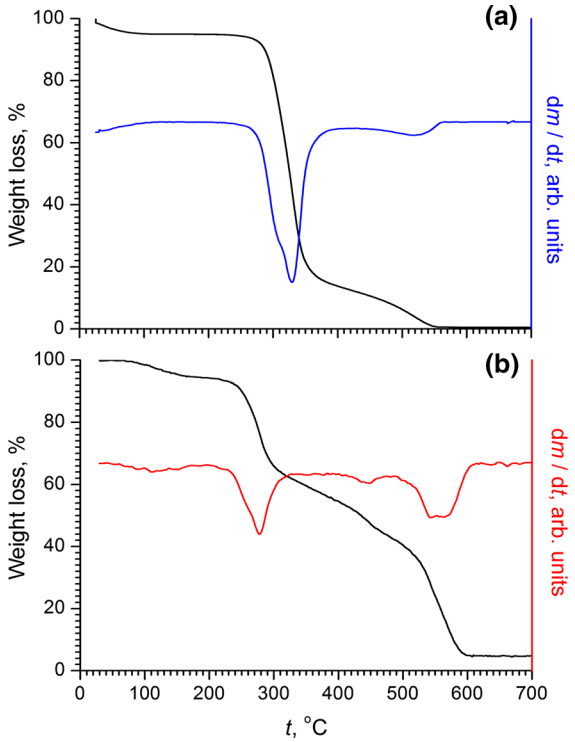

Fig. 3 TGA and DTG curves of **a** bare nanocellulose and **b** CNC/WO_3 films

formation of a number of intermediate tungsten-containing compounds, e.g., low tungsten oxides, oxycarbides, and carbides (see, e.g., Xiao et al. 2002; Bazarjani et al. 2014).

The third decomposition range (400–600 °C) in both samples can be attributed to the oxidation of the residual carbon (Teixeira et al. 2010). The weight loss data allowed the estimating of WO_3 content in CNC/WO_3 material (4.5 wt%). Thus, the obtained hybrid CNC/WO_3 film demonstrates a good thermal stability up to 200 °C, which allows it to withstand the harsh conditions during the medical sterilization procedure.

Photochromic properties of CNC/WO_3 films

Tungsten oxide is known to exhibit photochromic properties due to W^{6+} to W^{5+} reduction upon UV-irradiation (Wang et al. 2018). In the present work, the photochromic properties and the reversibility of photochromism for the freshly prepared hybrid CNC/WO_3 film, as well as the storage of the film for a long period of time (6 months under ambient conditions), were studied. The photochromic

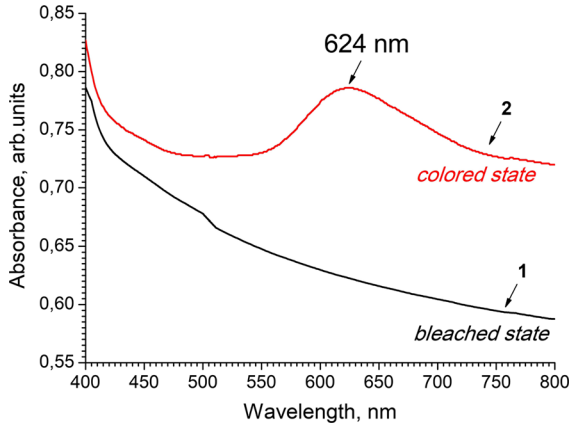

Fig. 4 UV–visible absorption spectra of UV-irradiated CNC/WO_3 film (1) in the bleached state and (2) after 1 min of UV-irradiation at 324 nm

coloration of the film was initiated by UV-irradiation (6 W UV lamp) and the bleaching of the film occurred upon its storage in the dark. Upon UV-irradiation, the CNC/WO_3 film changed its color from pale yellow into dark blue within approximately 1 min (see Fig. 4). In the dark, the colored CNC/WO_3 film gradually bleached back to its initial color within approximately 20 min (Fig. 4). The first visible signs of the coloration could be detected visually after 30 s of UV-irradiation. It should be noted that WO_3 sol used for the nanocellulose modification demonstrates a quicker color-bleaching transition, compared to the film. In particular, after 15 s of UV-irradiation the color of WO_3 sol becomes dark blue and returns to its original state in the dark within 3 min (Fig. 5a).

Interestingly, pure WO_3 sol demonstrated very poor reversibility in the coloration/bleaching process. As can be seen from Fig. 5a, the reversibility of the WO_3 sol coloration significantly decreases after 5 cycles. In turn, CNC/WO_3 film demonstrates excellent reversibility of color switching without any notable loss of efficiency after 10 cycles. The reversibility of photochromism of WO_3 in the hybrid nanocellulose film was additionally investigated after 6 months of the film storage. Compared to the freshly prepared film, stored film shows slower but still highly reversible coloration/bleaching. The overall bleaching process in this case takes more than 50 min (Fig. S1). Moreover, the duration of the bleaching increases when the number of cycles is increased. Interestingly, moisturizing the hybrid CNC/WO_3 film stored by 6 months with water vapor allows the restoration of its

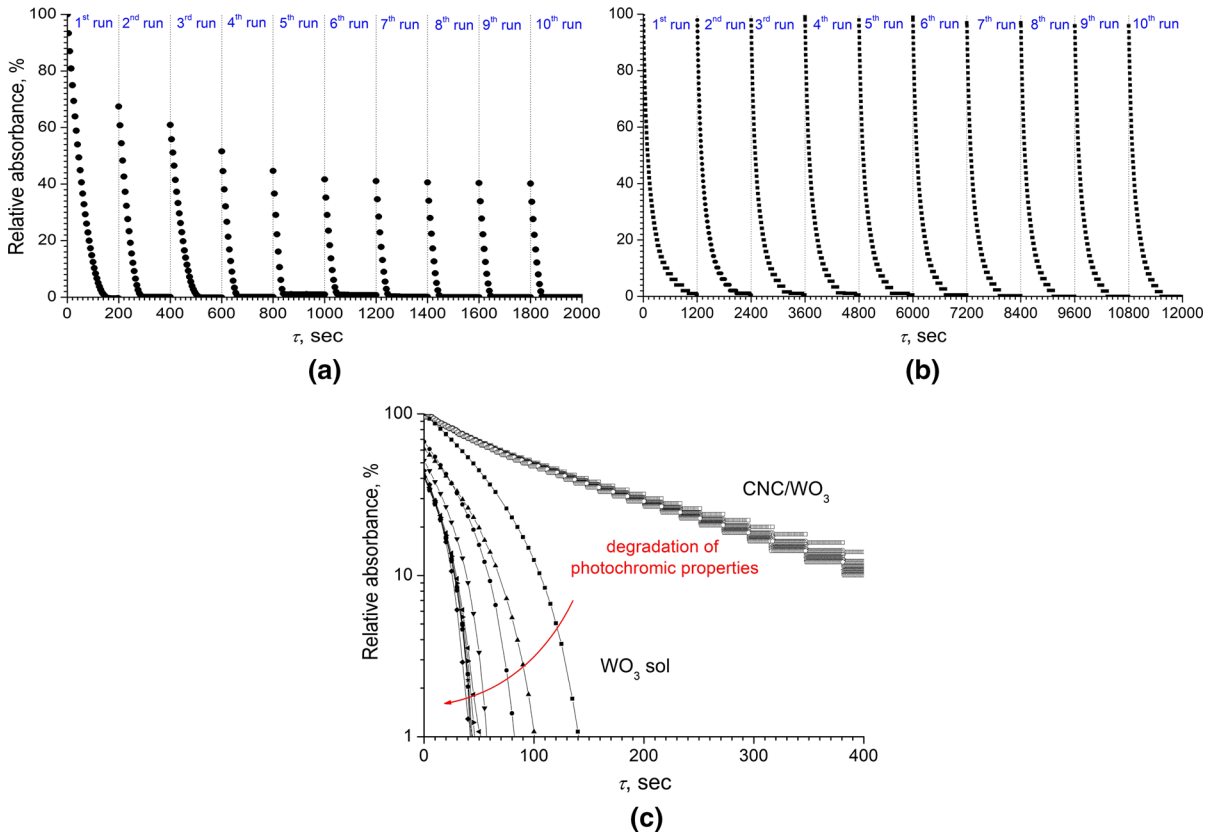

Fig. 5 The changes in the relative intensity of the absorption peak (624 nm) of UV-irradiated **a** WO_3 sol; **b** CNC/WO_3 film. **c** Comparison of the changes in the relative intensity of the absorption peak (624 nm) for UV-irradiated WO_3 sol and CNC/WO_3 film during 10 runs. Relative absorbance is given in log scale for visual clarity

initial photochromic behavior (Fig. S2). In particular, moisturized CNC/WO_3 film after UV irradiation shows gradual bleaching to its initial color within approximately 20 min.

Thus, introducing WO_3 nanoparticles into the biopolymer matrix allows stabilization and extension of the photochromic coloration reversibility. The use of both nanocellulose as an organic matrix and polyvinylpyrrolidone (PVP) as a stabilizer provide excellent reproducible photochromic properties of WO_3 nanoparticles upon UV irradiation. The mechanism of the photochromic behavior of tungsten oxide can be associated with the photoexcitation of the O → W ligand-to-metal charge transfer (LMCT) band (Yamase 1998). Earlier, Hwang et al. (2004) found that the compounds with the –OH groups enhance tungsten oxide photochromism. Adachi et al. (2012) confirmed this conclusion on the example of cellulose; photoreduction preferentially occurs for W^{6+} ions in the WO_3 matrix, which are bonded to the cellulose substrate via –OH hydrogen bonds. During the photochromic process, intervalence charge transfer (IVCT, $W^{+6} \rightarrow W^{+5}$) between tungsten oxide nanoparticles and polyglucan matrix occurs, which was supposed to be the major cause of the photochromic effect (Jing et al. 2014). Photoexcitation of WO_3 leads to the transfer of electron density from the oxygen atom to the tungsten atom (O_{2p}–W_{5d}) (Fig. 6).

On the other hand, nitrogen-containing compounds are more effective promoters of tungsten oxide photochromism, since nitrogen is a stronger electron donor. Thus, PVP not only acts as a good stabilizer of WO_3 nanoparticles, but also provides superior photochromic properties (Popov et al. 2018; He and Yao 2006) (Fig. 7).

Some authors have claimed that the formation of charge transfer complexes does not lead to the oxidation of PVP, while others have argued that PVP is oxidized in the course of tungsten oxide coloration, due to the electron transfer between the organic matrix

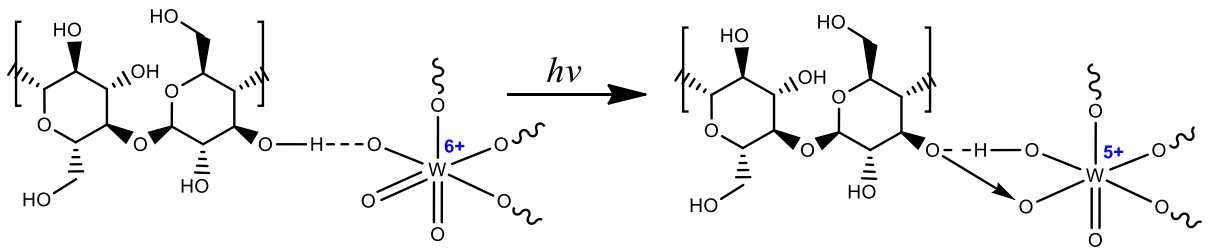

Fig. 6 The proposed mechanism of the electron density transfer from the oxygen atom in the CNC matrix to the tungsten atom

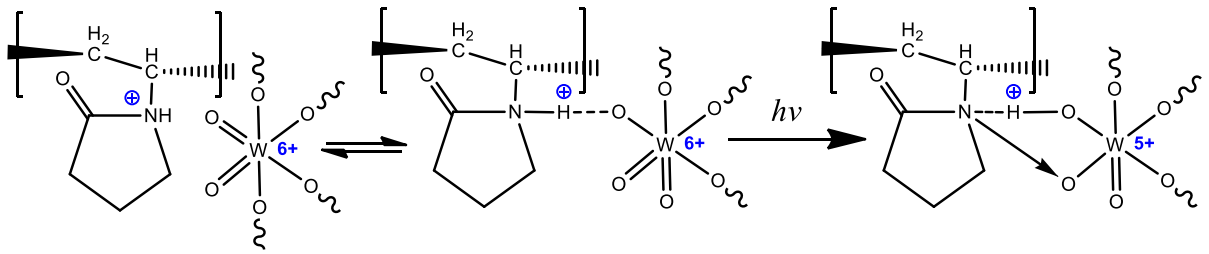

Fig. 7 The possible mechanism of the electron density transfer from the nitrogen atom of the PVP molecule to the tungsten atom

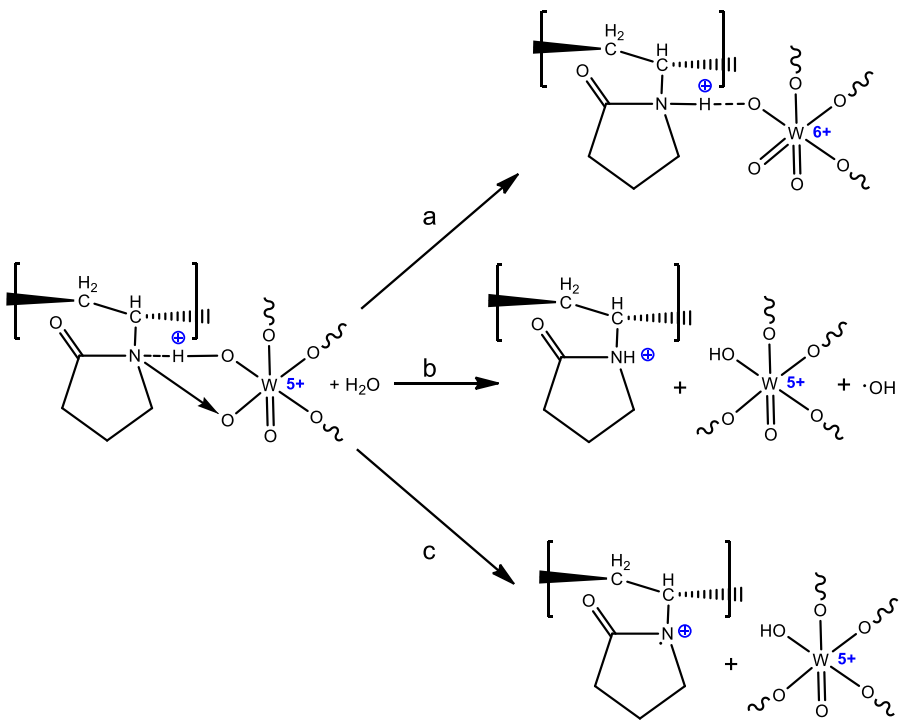

Fig. 8 The mechanism of the relaxation process of the colored LMCT complex, according to the model proposed by Yamase (1998)

and the metal anion (Ling et al. 2017). It is reasonable to assume that the deterioration of photochromism reversibility during the coloration/bleaching cycles of pure WO_3 sol can be explained by the destruction of PVP. Contrarily, in the nanocellulose matrix, this process can be compensated by polyglucan degradation, which occurs more readily, protecting the primary stabilizer. According to the mechanism proposed by Yamase (1998), the relaxation process of the colored LMCT complex leads to non-

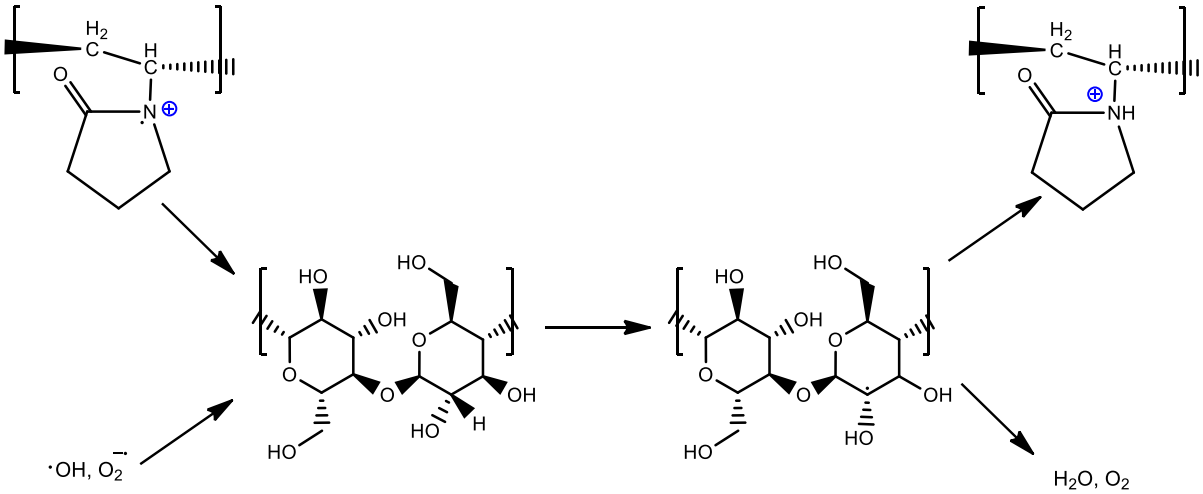

Fig. 9 The possible mechanism of ROS scavenging and PVP regeneration in the matrix of polyglucan

destructive bleaching (a), formation of highly aggressive ROS, namely a hydroxyl radical (b), and the decomposition of alkylammonium cation via a radical pathway (c) (Fig. 8).

Oxygen molecules accelerate the bleaching of the colored WO_3-containing composite, which may occur through electron transfer from the metal ion with a lower oxidation state (W^{+5}) to the oxygen molecule (He and Yao 2006), forming other active ROS, namely superoxide anion-radical: $O_2 + W^{+5} \rightarrow O_2^{-\cdot} + W^{+6}$. However, all the radicals formed can be inactivated by polyglucans, so that PVP remains unaltered (Fig. 9).

Moreover, since the proposed hybrid nanocellulose-based material contains many structural –OH groups, a sufficient amount of protons is available to intercalate into WO_6 moieties of tungsten oxide nanoparticles for charge compensation, preventing rapid spontaneous oxidation and stabilizing the blue coloration.

Conclusions

Hybrid nanocellulose/WO_3 films were produced by the simple and low-cost solvent casting method. The obtained films showed quick color-bleaching transition with a good reversibility of color switching after 10 cycles. The photochromism of the films was preserved upon long-term storage. The possible mechanisms of the photochromic reversibility were proposed. The hybrid nanocellulose/WO_3 films are believed to have great potential as a highly efficient low-cost photochromic material, with an easily scaled-up method of preparation.

Acknowledgments The work was supported by the Russian Science Foundation (Grant No. 18-73-10150). The electron microscopy and energy-dispersive X-ray spectroscopy measurements were performed using shared experimental facilities supported by IGIC RAS state assignment.

Compliance with ethical standards

Conflicts of interest There are no conflicts of interest to declare.

References

Adachi K, Mita T, Tanaka S, Honda K, Yamazaki S, Nakayama M, Goto T, Watara H (2012) Kinetic characteristics of enhanced photochromism in tungsten oxide nanocolloid adsorbed on cellulose substrates, studied by total internal reflection Raman spectroscopy. RSC Adv 2:2128–2136. https://doi.org/10.1039/c2ra00217e

Bartha L, Kiss AB, Szalay T (1995) Chemistry of tungsten oxide bronzes. Int J Refract Met Hard Mater 13:77–91. https://doi.org/10.1016/0263-4368(94)00031-X

Bazarjani MS, Müller MM, Kleebe H-J, Fasel C, Riedel R, Gurlo A (2014) In situ formation of tungsten oxycarbide, tungsten carbide and tungsten nitride nanoparticles in micro- and mesoporous polymer-derived ceramics. J Mater Chem A 2:10454–10464. https://doi.org/10.1039/C4TA01509F

Chinde S, Dumala N, Rahman MF, Kamal SSK, Kumari SI, Mahboob M, Grover P (2017) Toxicological assessment of tungsten oxide nanoparticles in rats after acute oral

exposure. Environ Sci Pollut Res 24(15):13576–13593. https://doi.org/10.1007/s11356-017-8892-x

Dejournett TJ, Spicer JB (2014) The influence of oxygen on the microstructural, optical and photochromic properties of polymer-matrix, tungsten-oxide nano-composite films. Sol Energy Mater Sol Cell 120:102–108. https://doi.org/10.1016/j.solmat.2013.08.023

Ding D, Shen Y, Ouyang Y, Li Z (2012) Hydrothermal deposition and photochromic performances of three kinds of hierarchical structure arrays of WO_3 thin films. Thin Solid Films 520:7164–7168. https://doi.org/10.1016/j.tsf.2012.08.003

Dong H, Snyder JF, Tran DT, Leadorea JL (2013) Hydrogel, aerogel and film of cellulose nanofibrils functionalized with silver nanoparticles. Carbohydr Polym 95(2):760–767. https://doi.org/10.1016/j.carbpol.2013.03.041

Evdokimova OL, Svensson FG, Agafonov AV, Håkansson S, Seisenbaeva GA, Kessler VG (2018) Hybrid drug delivery patches based on spherical cellulose nanocrystals and colloid titania-synthesis and antibacterial properties. Nanomaterials 8(4):228. https://doi.org/10.3390/nano8040228

Faustini M, Nicole L, Ruiz-Hitzky E, Sanchez C (2018) History of organic-inorganic hybrid materials: prehistory, art, science, and advanced applications. Adv Funct Mater 28(27):1704158. https://doi.org/10.1002/adfm.201704158

Han B, Popov AL, Shekunova TO, Kozlov DA, Ivanova OS, Rumyantsev AA, Shcherbakov AB, Popova NR, Baranchikov AE, Ivanov VK (2019) Highly crystalline WO_3 nanoparticles are non-toxic to stem cells and cancer cells. J Nanomater 2019:5384132. https://doi.org/10.1155/2019/5384132

He T, Yao J (2006) Photochromism in composite and hybrid materials based on transition-metal oxides and polyoxometalates. Prog Mater Sci 51(6):810–879. https://doi.org/10.1016/j.pmatsci.2005.12.001

Henrique MA, Neto WPF, Silvério HA, Martins DF, Gurgel LVA, da Silva Barud H, de Morais LC, Pasquini D (2015) Kinetic study of the thermal decomposition of cellulose nanocrystals with different polymorphs, cellulose I and II, extracted from different sources and using different types of acids. Ind Crops Prod 76:128–140. https://doi.org/10.1016/j.indcrop.2015.06.048

Hosseini F, Rasuli R, Jafarian V (2018) Immobilized WO_3 nanoparticles on graphene oxide as a photo-induced antibacterial agent against UV-resistant *Bacillus pumilus*. J Phys D Appl Phys 51(14):145403. https://doi.org/10.1088/1361-6463/aab1a6

Hwang DK, Kim HJ, Han HS, Shul YG (2004) Development of photochromic coatings on polycarbonate. J Sol Gel Sci Technol 32(1–3):137–141. https://doi.org/10.1007/s10971-004-5778-4

Jakhmola A, Anton N, Anton H, Messaddeq N, Hallouard F, Klymchenko A, Mely Y, Vandamme TF (2014) Poly-ε-caprolactone tungsten oxide nanoparticles as a contrast agent for X-ray computed tomography. Biomaterials 35(9):2981–2986. https://doi.org/10.1016/j.biomaterials.2013.12.032

Jing X, Zou D, Meng Q, Zhang W, Zhang F, Feng W, Han X (2014) Fabrication and visible-light photochromism of novel hybrid inorganic–organic film based on polyoxometalates and ethyl cellulose. Inorg Chem Commun 46:149–154. https://doi.org/10.1016/j.inoche.2014.05.030

Kalhori H, Ranjbar M, Salamati H, Coey JMD (2016) Flower-like nanostructures of WO_3: fabrication and characterization of their in-liquid gasochromic effect. Sens Actuators B 225:535–543. https://doi.org/10.1016/j.snb.2015.11.044

Kaushika M, Moores A (2016) Review: nanocelluloses as versatile supports for metal nanoparticles and their applications in catalysis. Green Chem 18:622–637. https://doi.org/10.1039/C5GC02500A

Kim SJ, Choi SJ, Jang JS, Kim NH, Hakim M, Tuller HL, Kim I-D (2016) Mesoporous WO_3 nanofibers with protein-templated nanoscale catalysts for detection of trace biomarkers in exhaled breath. ACS Nano 10:5891–5899. https://doi.org/10.1021/acsnano.6b01196

Kuribara K, Wang H, Uchiyama N, Fukuda K, Yokota T, Zschieschang U, Jaye C, Fischer D, Klauk H, Yamamoto T, Takimiya K, Ikeda M, Kuwabara H, Sekitani T, Loo Y-L, Someya T (2012) Organic transistors with high thermal stability for medical applications. Nat Commun 3:723. https://doi.org/10.1038/ncomms1721

Ling Z, Chen S, Zhang X, Takabe K, Xu F (2017) Unraveling variations of crystalline cellulose induced by ionic liquid and their effects on enzymatic hydrolysis. Sci Rep 7:10230. https://doi.org/10.1038/s41598-017-09885-9

Nandiyanto ABD, Arutanti O, Ogi T, Iskandar F, Kim TO, Okuyama K (2013) Synthesis of spherical macroporous WO_3 particles and their high photocatalytic performance. Chem Eng Sci 101:523–532. https://doi.org/10.1016/j.ces.2013.06.049

Poletto M, Ornaghi Júnior HL, Zattera AJ (2014) Native cellulose: structure, characterization and thermal properties. Materials 7:6105–6119. https://doi.org/10.3390/ma7096105

Popov AL, Zholobak NM, Balko OI, Balko OB, Shcherbakov AB, Popova NR, Ivanova OS, Baranchikov AE, Ivanov VK (2018) Photo-induced toxicity of tungsten oxide photochromic nanoparticles. J Photochem Photobiol B 178:395–403. https://doi.org/10.1016/j.jphotobiol.2017.11.021

Reddy JP, Rhim J-W (2014) Characterization of bionanocomposite films prepared with agar and paper-mulberry pulp nanocellulose. Carbohydr Polym 110:480–488. https://doi.org/10.1016/J.CARBPOL.2014.04.056

Shekunova TO, Baranchikov AE, Yapryntsev AD, Rudakovskaya PG, Ivanova OS, Karavanova YuA, Kalinina MA, Rumyantseva MN, Dorofeev SG, Ivanov VK (2018) Ultrasonic disintegration of tungsten trioxide pseudomorphs after ammonium paratungstate as a route for stable aqueous sols of nanocrystalline WO_3. J Mater Sci 53(3):1758–1768. https://doi.org/10.1007/s10853-017-1668-3

Shen PK, Huang HT, Tseung ACC (1992) A study of tungsten trioxide and polyaniline composite films: I. Electrochemical and electrochromic behavior. J Electrochem Soc 139:1840–1845. https://doi.org/10.1149/1.2069508

Shi Z, Phillips GO, Yang G (2013) Nanocellulose electroconductive composites. Nanoscale 5:3194–3201. https://doi.org/10.1039/c3nr00408b

Siciliano T, Tepore A, Micocci G, Serra A, Manno D, Filippo E (2008) WO_3 gas sensors prepared by thermal oxidization of tungsten. Sens Actuators B 133(1):321–326. https://doi.org/10.1016/j.snb.2008.02.028

Siqueira G, Bras J, Dufresne A (2010) Cellulosic bionanocomposites: a review of preparation, properties and applications. Polymers 2(4):728–765. https://doi.org/10.3390/polym2040728

Stoenescu S, Badilescu S, Sharma T, Brüning R, Truong V-V (2016) Tungsten oxide–cellulose nanocrystal composite films for electrochromic applications. Opt Eng 55(12):127102. https://doi.org/10.1117/1.OE.55.12.127102

Tahir MB, Nabi G, Rafique M, Khalid NR (2017) Nanostructured-based WO_3 photocatalysts: recent development, activity enhancement, perspectives and applications for wastewater treatment. Int J Environ Sci Technol 14:2519–2542. https://doi.org/10.1007/s13762-017-1394-z

Teixeira EM, Oliveira CR, Mattoso LHC, Corrêa AC, Paladin PD (2010) Nanofibras de algodão obtidas sob diferentes condições de hidrólise ácida. Polámeros 20:264–268. https://doi.org/10.1590/S0104-14282010005000046

Thummavichai K, Xia Y, Zhu Y (2017) Recent progress in chromogenic research of tungsten oxides towards energy-related applications. Progr Mater Sci 88:281–324. https://doi.org/10.1016/j.pmatsci.2017.04.003

Wang S, Fan W, Liu Z, Yu A, Jiang X (2018) Advances on tungsten oxide based photochromic materials: strategies to improve their photochromic properties. J Mater Chem C 6:191–212. https://doi.org/10.1039/C7TC04189F

Xiao T, Hanif A, York APE, Sloan J, Green MLH (2002) Study on preparation of high surface area tungsten carbides and phase transition during the carburization. Phys Chem Chem Phys 4:3522–3529. https://doi.org/10.1039/B202518C

Yamase T (1998) Photo- and electrochromism of polyoxometalates and related materials. Chem Rev 98(1):307–326. https://doi.org/10.1021/cr9604043

Yamazaki S, Yamate T, Adachi K (2013) Photocatalytic activity of aqueous WO_3 sol for the degradation of orange II and 4-chlorophenol. Appl Catal A 454:30–36. https://doi.org/10.1016/j.apcata.2012.12.038

Yamazaki S, Ishida H, Shimizu D, Adachi K (2015) Photochromic properties of tungsten oxide/methylcellulose composite film containing dispersing agents. ACS Appl Mater Interfaces 7(47):26326–26332. https://doi.org/10.1021/acsami.5b09310

Yassin AM, Elnouby M, El-Deeb NM, Hafez EE (2016) Tungsten oxide nanoplates; the novelty in targeting metalloproteinase-7 gene in both cervix and colon cancer cells. Appl Biochem Biotechnol 180(4):623–637. https://doi.org/10.1007/s12010-016-2120-x

Zhang B, Liu R, Pan Y, Wang Q, Liu B (2018) Cellulose-based WO3 nanocomposites prepared by a sol–gel method at low temperature. IOP Conf Ser Mater Sci Eng 301:012075. https://doi.org/10.1088/1757-899x/301/1/012075

Zhao Y, Yan X, Yang KR, Cao S, Dong Q, Thorne JE, Materna KL, Zhu S, Pan X, Flytzani-Stephanopoulos M, Brudvig GW, Batista VS, Wang D (2018) End-on bound iridium dinuclear heterogeneous catalysts on WO_3 for solar water oxidation. ACS Cent Sci 4(9):1166–1172. https://doi.org/10.1021/acscentsci.8b00335

Zheng H, Ou JZ, Strano MS, Kaner RB, Mitchell A, Kalantar-zadeh K (2011) Nanostructured tungsten oxide—properties, synthesis, and applications. Adv Funct Mater 21(12):2175–2196. https://doi.org/10.1002/adfm.201002477